Talanta 118 (2014) 321–327

Contents lists available at ScienceDirect

Talanta

journal homepage: www.elsevier.com/locate/talanta

Characterization of stainless steel assisted bare gold nanoparticles and their analytical potential

A.I. López-Lorente [a,b], B.M. Simonet [a], M. Valcárcel [a,*], S. Eppler [b], R. Schindl [b], C. Kranz [b], B. Mizaikoff [b]

[a] Department of Analytical Chemistry, University of Córdoba, E-14071 Córdoba, Spain
[b] Institute of Analytical and Bioanalytical Chemistry, University of Ulm, Ulm, Germany

ARTICLE INFO

Article history:
Received 14 June 2013
Received in revised form
2 October 2013
Accepted 15 October 2013
Available online 24 October 2013

Keywords:
Bare gold nanoparticles
Stainless steel
Synthesis
Characterization
Surface enhanced Raman spectroscopy
Carbon nanotubes

ABSTRACT

A simple, environmentally friendly, one-pot method to synthesize highly stable bare gold nanoparticles (AuNPs) has been developed. AuNPs have been synthesized from tetrachloroauric acid solution using steel or stainless steel as solid reducing agent, which can be reused. The proposed method yields bare gold nanoparticles at atmospheric pressure and room temperature for potentially producing large quantities. The obtained AuNPs have been characterized by SEM, TEM and AFM finding an average diameter of around 20 nm, polygonal yet nearly spherical shape and a narrow size distribution. The mechanism of reaction has been investigated by UV–vis spectroscopy, ICP-OES and EDX analysis. The obtained dispersed gold nanoparticles proved to be stable if stored a 4 °C for over four months without the addition of a stabilizing agent. Their analytical potential as SERS substrate has been demonstrated and their performance compared with that showed by citrate-coated gold nanoparticles. Thanks to their unique properties, their use as analytical tools provides analytical processes with enhanced selectivity and precision.

1. Introduction

Noble metal nanoparticles – gold nanoparticles (AuNPs) being included among them – have arouse great attention, offering huge potential for their application in fields such as nanomedicine and nanotechnologies as they provide several opportunities in imaging, diagnostics, and therapies [1,2].

In general, the synthetic routes leading to nanoparticles can be grouped into top-down and bottom-up strategies. In the so-called top-down approaches, nanoparticles are directly generated from bulk materials via the generation of isolated atoms usually involving physical methods such as milling, attrition, repeated quenching and photolithography [3]. Bottom-up strategies comprise molecular components as starting materials linked with chemical reactions, nucleation and growth process to promote the formation of clusters. Usually, they rely on the chemical reduction of metal salts, electrochemical pathways, or the controlled decomposition of metaestable organometallic compounds [4].

Among all the methods described, colloidal gold is most often prepared by reduction of gold halides (for example $HAuCl_4$) with the use of chemical reducing agents in solution such as sodium citrate [5–7] – also in the presence of tannin [8,9] –, sodium borohydride [10,11], ascorbic acid [12], ethylenediaminetetraacetic acid (EDTA) [13] or cyanoborohydride [14], which usually requires stabilizers or ligands. In most of these cases, the solution will be composed by the metallic particle, a counterion, the reductant or its byproducts (such as ketoglutaric acid for example in the case of citrate reduction [15]) and, in some cases, an organic stabilizer. The presence of those adsorbates may affect the optical characteristics of nanoparticles [16] as well as their photochemical reactivity [17], limiting future functionalizations [18] and causing interferences in citotoxicity studies [19]. Moreover, chemicals employed for both reduction or stabilization of nanoparticles can be waste pollutants [20]. In the last years, several so-called “green” synthetic methods involving the use of plant extracts as well as microorganism have been proposed [21,22].

While less commonly applied, bare gold nanoparticles without impurities within the metal particle surface have been also synthesized via physical (based on ultrasonic, UV, IR or ionizing radiation or laser photolysis) [23–26] and electrochemical methods [27]. The advantages of those methods are that impurities of chemical compounds are absent on the metal particle surface.

Laser ablation has been used for the synthesis of gold nanoparticles in liquid solution [26,28], obtaining AuNPs without chemical reagents or ligands. Those particles are electrically

* Corresponding author. Tel./fax: +34 957 218616.
E-mail addresses: qa1meobj@uco.es (M. Valcárcel), boris.mizaikoff@uni-um.de (B. Mizaikoff).

0039-9140/$ - see front matter © 2013 Elsevier B.V. All rights reserved.
http://dx.doi.org/10.1016/j.talanta.2013.10.028

charged, thus, the resulting solution being stable for up to several months. However, it does not allow good control of size and size distribution. The formation of colloidal unmodified gold nanoparticles has been also achieved by irradiation of a precursor solution with X-rays from a synchrotron source, without the need of pre-added stabilizers [29]. Furthermore, gold nanoparticles have been produced by H_2 reduction of Au(III) oxide without any addition of stabilizer or counterion other than the metal ions and water dissociation ions [30].

This study demonstrates the possibility to synthesize bare gold nanoparticles (AuNP) from tetrachloroauric acid solution using steel or stainless steel as solid reducing agent. This green method avoids the use of a reductant in solution. Furthermore, the proposed synthesis method yields bare AuNPs at atmospheric pressure and room temperature for potentially producing large quantities, whereas the methods described to date to achieve nanoparticles without ligands usually require more complex instrumentation or reaction conditions such as e.g., molecular hydrogen at a pressure slightly higher than atmospheric conditions [30]. The analytical potential of these bare gold nanoparticles has been demonstrated for their use as substrates in surface enhanced Raman scattering (SERS) spectroscopic determination of carboxylated single walled carbon nanotubes (c-SWNTs).Their performance has been compared with that of gold nanoparticles reduced by citrate.

2. Experimental

2.1. Materials and reagents

$HAuCl_4$ (Sigma Aldrich) was used to synthesize the gold nanoparticles. Before synthesis the material were washed with a mixture of nitric acid and hydrochloric acid (PANREAC). 1,10-phenantrolin was purchased from VWR (Germany). Sodium citrate dihydrate 99.5% (Sigma Aldrich) were used to synthesize citrate-coated gold nanoparticles in order to be compared with those obtained with the proposed method. A flat piece of 304-stainless steel was employed as solid reductant of gold salt in order to form gold nanoparticles.

Single walled carbon nanotubes (SWNTs) used to investigate SERS properties of synthesized nanoparticles were purchased from Shenzhen Nanotech Port Co. Ltd (NTP) (China), with a purity over 90%, an outer diameter of <2 nm, a length of 5–15 μm and a special surface area of 500–700 m^2/g. Acetate of cellulose membranes of 0.2 μm pore size were purchased from Sartorius Stedim Biotech (Germany).

2.2. Equipments

Characterization of the nanoparticles was performed using an AFM 5500 by Agilent equipped with NCL-W Point probe-Silicon SPM-cantilevers. For AFM studies of AuNPs, a piece of silicon wafer was covered with AuNP suspension, dried, and then imaged by AFM in tapping mode with a resonance frequency of 190 kHz and a force constant of 48 N m^{-1}. SEM measurements were performed with a Quanta 3D FEG, FEI Company (Eindhoven, Nederland) equipped with an energy dispersive x-ray spectroscopy (EDX) detector. TEM images were recorded using a PHILIPS CM-10 system. UV/Vis measurements were performed using a halogen lamp as light source, and a monocromator combined with a photonic detector of a PTI Fluoresecence Master System as detector. In order to investigate the mechanism of the reaction and the involved constituents an Ultima2 Horiba Jobin Yvon ICP-OES was used.

Raman measurements were performed with a portable Raman spectrometer system (inno-Ram) from B&W TEK Inc. with a wavelength of 785 nm and a maximum laser output power of 285 mW in the probe. Laser power was set to 5.7 mW for measurements, using a 1 s acquisition and accumulating a total of 10 spectra.

2.3. Stainless steel assisted synthesis of bare gold nanoparticles

Gold nanoparticles were synthesized by a novel method, which is based on the reduction of the $HAuCl_4$ mediated by stainless steel at ambient conditions. All glassware were cleaned with freshly prepared aqua regia (HNO_3:HCl 1:3 mixture) and then rinsed thoroughly with distilled H_2O prior to use. A piece of 304-stainless steel (129 mm^2 of total surface) was introduced into 100 μL of a 0.2 mg mL^{-1} aqueous solution of $HAuCl_4$. The reaction is carried out at room temperature and the stainless steel substrate was simultaneously used as stirrer during the reaction. By increasing the temperature, the reaction is significantly accelerated. Higher concentrations of $HAuCl_4$ have also been tested; a 10-fold higher concentrated $HAuCl_4$ solution (2 mg mL^{-1}) leads to more rapidly obtaining gold nanoparticles, yet, the stability of the solution is reduced.

It should be noted that both steel and stainless steel may act as reducing agent. Due to its utility and availability, the current study was limited to stainless steel as solid reducing agent.

2.4. Synthesis of gold nanoparticles by citrate reduction

Gold nanoparticles obtained via $HAuCl_4$ reduction mediated by sodium citrate were also prepared according to the method described by Turkevich et al. [5] with some modifications as described elsewhere [31]. All glassware were cleaned with freshly prepared aqua regia (HNO_3:HCl 1:3 mixture) and then rinsed thoroughly with distilled H_2O prior to use. $HAuCl_4$ and sodium citrate solutions were filtered through a 0.45 μm nylon membrane prior use. 0.254 mL of a 15 sodium citrate solution were added to a 0.01% boiling solution of HAuCl4. The system was then left to react while being stirred for 15 min. Afterwards, 5 mL of 0.01% $HAuCl_4$ solution were added to the system followed by 0.254 mL of 1% sodium citrate solution and it was stirred at heating for 15 min. Then the heater was switched off and the solution was kept stirred until cool to room temperature. Gold nanoparticles were stored at 4 °C in an amber bottle.

2.5. SERS measurements

In order to prove the analytical potential of these nanoparticles obtained through the proposed procedure, SERS spectra of carboxylated single walled carbon nanotubes were measured. Carboxylated carbon nanotubes (c-SWNTs) were prepared by adding 100 mg of SWNTs to 20 mL of 3:1 H_2SO_4/HNO_3 mixture in a glass flask, as described elsewhere [32]. After refluxed for 1 h, c-SWNTs were washed with water and centrifuged at 10,062*g* for 10 min until the pH were neutral. Finally, carboxylated carbon nanotubes were dried in a heater set at 60 °C. Carboxylic groups present in nanotube sidewalls and open ends provide them solubility in water.

SERS measurements were carried out by depositing 10 μL of gold nanoparticles solution on acetate of cellulose membrane (pore size of 0.2 μm) by using a home-made filtration device with a filtration diameter of 1.3 mm. Then, aqueous stock solutions of c-SWNTs were filtered and nanotubes adsorbed on previously deposited gold nanoparticles. The intensity of carbon nanotubes G band around 1583 cm^{-1} was selected as analytical signal to prove the suitability of bare gold nanoparticles as SERS substrate.

3. Results and discussion

3.1. UV–vis spectroscopic characterization

If steel or stainless steel is inserted into a tetrachloroauric acid solution, the homogenous formation of gold nanoparticles in solution is observed along with a small amount of AuNPs formed at the surface of the solid reducing agent. The kinetics of the synthesis of AuNPs may be directly observed via UV/Vis spectroscopy in a cuvette (Fig. 1) since gold nanoparticles provide a characteristic absorption due to their plasmon resonance bands [33]. The solution was stirred at low velocity in order to assure homogeneity. The own stainless steel acts as stir bar as the synthesis of the nanoparticles takes place in a vial placed on a magnetic stirrer.

As can be seen in Fig. 1, the reaction is almost completed after 70 min when it is performed at room temperature (~20 °C). In addition to the UV/Vis spectra evolution shown in Fig. 1, in order to corroborate the quantitative production of gold nanoparticles, synthesized gold nanoparticles were centrifuged at 10,062*g*. Then, the supernatant was analyzed showing no absorption at around 320 nm typical of Au(III) species (visually it can be also observed that the yellowish colour typical of Au(III) was not present).

The influence of temperature on the performance of the synthesis was studied. It was found that when temperature was increased until 70 °C, the reaction was accelerated to only 15 min until completion. Fig. 2 (top) also depicts the dependence of formation rate of gold nanoparticles at four different temperatures, namely: 25, 40, 70 and 85 °C. As can be seen, the absorbance intensity of gold nanoparticles solutions for a reaction time of 3 min increases linearly when increasing temperature, which means that nanoparticles are being synthesized faster and a higher concentration of them are present in solutions at higher temperature for a certain time in comparison with those at lower temperatures.

Moreover, the effect of pH was studied in the range of 2.6–6.37. The chemical stability of $HAuCl_4$ constitutes the high pH limit. Fig. 2 (bottom) shows the behavior observed, being low pH most appropriate to perform the synthesis since leads to high rates of formation of nanoparticles. A pH of 2.6 was selected for further experiments. As can be seen in Fig. 2, at pH 6.37 the formation of gold nanoparticles has not started after 3 min of reaction, probably due to Au(III) inestability. The pH of the solution was monitored during the synthesis of gold nanoparticles observing that pH value keeps almost constant around a value of 2 (using a starting $HAuCl_4$ solution of 200 mg dL^{-1}).

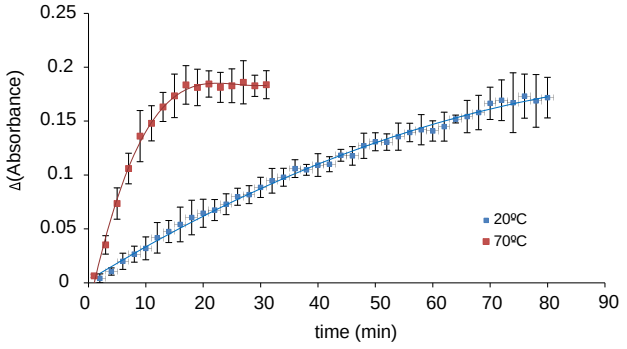

Fig. 1. Kinetics of the stainless steel assisted synthesis of AuNPs performed in a UV/V is cuvette under stirring at two different temperatures. The initial concentration of $HAuCl_4$ was 0.2 mg mL^{-1}. The graph represents the increment in absorbance of the maximum and the base of the peak.

3.2. Microscopic characterization

The obtained gold nanoparticles have been characterized by scanning electron microscopy (SEM), transmission electron microscopy (TEM), and atomic force microscopy (AFM) in order to determine their size and shape. From the TEM images, also the size distribution has been calculated (Fig. 3). The obtained AuNPs appear homogeneous in shape and size and of polygonal yet nearly spherical shape. Of particular interest is also the fact that thus obtained AuNPs are well dispersed with neither aggregates nor rods observed. The average diameter of the nanoparticles was determined to be 20 ± 6 nm.

AFM studies have confirmed the nominal colloid size for the obtained nanoscale particles (Fig. 4). The average size of the nanoparticles derived from AFM studies was 21 ± 9 nm, which is comparable to the results obtained using TEM.

3.3. Inductively coupled plasma atomic emission spectroscopy studies

Inductively coupled plasma optical emission spectroscopy (ICP-OES) was used to analyze which metals were present in solution after the synthesis. A systematic study of the solutions containing gold nanoparticles synthesized by introducing the stainless steel piece in a tetrachloroauric solution was performed at different pH values, as shown in Fig. 5. It was found that after Au–forming the nanoparticles- Fe is the dominant metal species complemented by trace levels of Cr, Ni, Mn, and Mo (Fig. 5).

Additionally, the release of metals from stainless steel in acidic conditions was investigated by using HCl solutions at different pH values. Fe was found to be also released from the stainless steel in higher concentration as low as pH is. This behavior is similar to that observed with $HAuCl_4$ solutions. Nevertheless, Fe concentrations found in the case of HCl at the same pH than $HAuCl_4$ are lower. Thus, the oxidative character of $AuCl_4^-$ ions may play a role in the oxidation of Fe.

3.4. Energy dispersive X-ray spectroscopic characterization

In order to investigate if metals released from the stainless steel surface are subsequently incorporated into the AuNPs, EDX studies were performed corroborating that the obtained nanoparticles were only composed of gold. When recording EDX spectra of AuNPs collected while the reaction is still in progress, gold salt residues are still evident as indicated by chlorine ions present within salt crystals. In contrast, EDX spectra collected at gold nanoparticles after the reaction was complete only revealed a gold line.

3.5. Proposed mechanism of the reaction

Stainless steel promotes the reduction of Au(III) to Au(0) as nanoparticles. ICP-OES analysis proved the release of metals from the stainless steel mesh. The oxidative character of $AuCl_4^-$ ions may play a significant role in their oxidation and excretion since higher amounts of Fe are released into a HAuCl4 solution as compared to neat HCl solution of the same pH. Once the stainless steel piece was analyzed by EDX, it was found that in addition to the formation of AuNPs in solution, a small amount of AuNPs were also formed at their surface.

In order to corroborate the hypothesis of the proposed reaction mechanism, a qualitative assay was performed adding 1,10-phenantrolin (a coloured redox indicator) to the solution during the synthesis, which results in the formation of an orange-coloured complex upon the insertion of the stainless steel substrate into the acidic solution of both HCl and $HAuCl_4$, which in turn confirms the release of Fe(II) into the solution. Thus, one possible mechanism of formation of AuNPs is

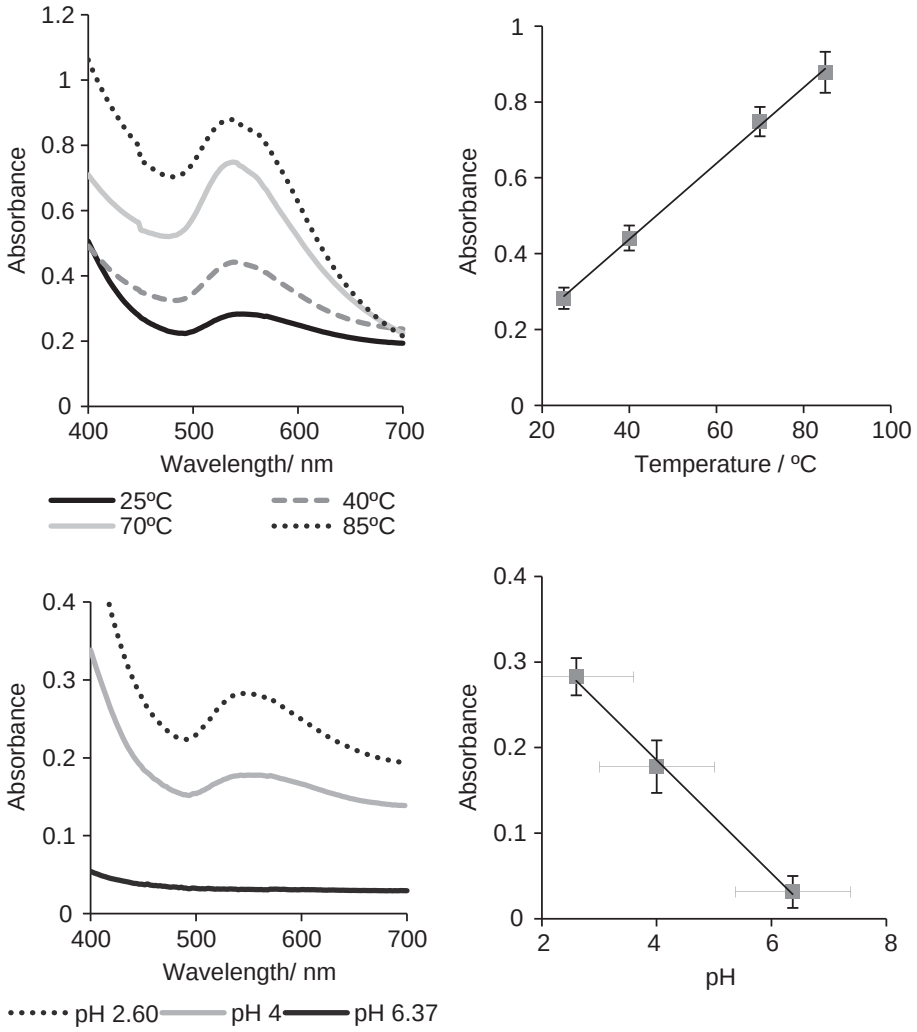

Fig. 2. Effect of temperature for a reaction time of 3 min (top): the left image depicts the absorbance band of gold nanoparticles solution measured 3 min after introducing the stainless steel piece into the tetrachloroauric solution, the right image show the linear dependence of the band height with temperature conditions. Influence of the pH in the reaction for a temperature of 40 °C and 3 min of reaction (bottom): left image shows UV–vis spectra of gold nanoparticles solutions synthesized at different pH conditions, the right image depicts the dependence of band height with pH.

the reduction of Au(III) by the electron liberated from the oxidation of stainless steel Fe(0) to Fe(II) in higher amounts as well as due to other metals (Ni,Cr) yet at to a lesser extent.

In addition, the efficiency of iron mesh to produce gold nanoparticles similarly to stainless steel production was proved. In this case, the reduction of Au(III) to Au(0) as a thin gold layer above the iron surface was observed, as previously reported [34], while stainless steel yields nanoparticles with a reproducible size instead of a gold layer. On the other hand, the reaction mainly occurs in the bulk of the solution. This fact leads to the hypothesis that hydrogen, which is formed as a consequence of the reduction of protons of the acidic media mediated by the steel substrate, reduces $AuCl_4^-$ ions yielding AuNPs (Fig. 6). The formation of gold nanoparticles via hydrogen has been previously described in literature [30], although it yields AuNPs that are significantly larger than those synthesized with the novel methodology presented herein. If we evaluate the potential of reduction of the pairs H^+/H_2 ($E=0$ V), Fe^{2+}/Fe^0 ($E=-0.440$ V), Ni^{2+}/Ni^0 ($E=-0.250$ V) and Cr^{2+}/Cr^0 ($E=-0.912$ V), it can be hypothesized that during the oxidation of these metals when released from the stainless steel the reduction of H^+ ions present in the acidic solution may take place. When monitoring the pH of the solution during the reaction we have observed that the pH was maintained almost constant during the formation of the gold nanoparticles at acidic value (around 2), thus -in order to maintain the pH value- H_2 formed may be oxidized again to H^+ while reducing the remaining Au(III) in solution. An evaluation of the potential of such reaction showed that this reaction could take place since $E(AuCl_4^-/Au)=1.002$ V and $E(H^+/H_2)=0$ V.

The performance of the reaction appears best for stainless steel as the generation of H_2 mediated by it appears to occur at just the right rate, and is lower than e.g., in the case of using iron metal, which leads to the formation of instable nanoparticles that do not remains in solution (data not shown).

If only H_2 is bubbled through a solution of $HAuCl_4$ in absence of a stainless steel substrate at ambient conditions, the reduction of Au(III) is observed, yet there is no formation of gold nanoparticles evident. Instead, if H_2 is bubbled through the solution in addition to inserting a stainless steel substrate, gold is reduced at the end of the polymer tube bubbling H_2 into the solution instead of generating AuNPs. Consequently, the release rate of H_2 mediated by stainless steel plays a crucial role for successfully synthesizing stable AuNPs at ambient conditions. Hence, we may summarize the reaction as

$$2HAuCl_4+3H_2\rightarrow 3Au\ (\text{nanoparticles})+8HCl \quad (1)$$

with a global standard redox potential of $\Delta E_o=1.002$ V, which implies that the reaction will spontaneously evolve (Fig. 6).

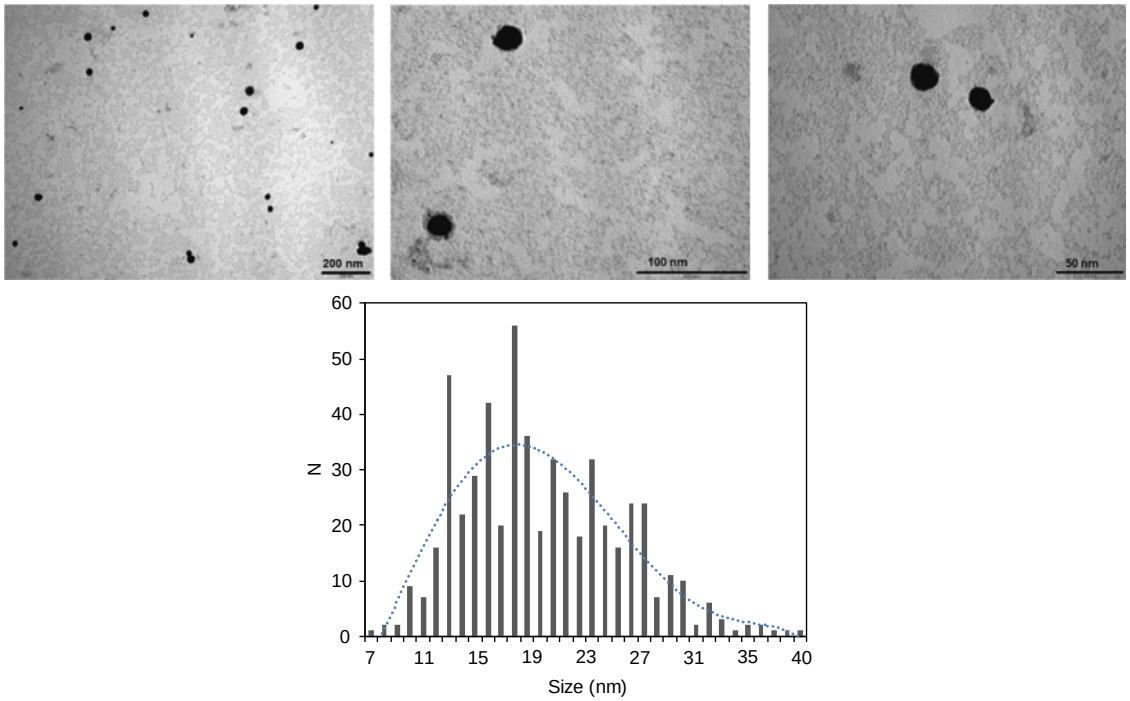

Fig. 3. Top: TEM images of collected individual gold nanoparticles obtained during stainless steel assisted synthesis. Bottom: Size distribution of the particles resulting in $d_{ave}=20\pm6$ nm.

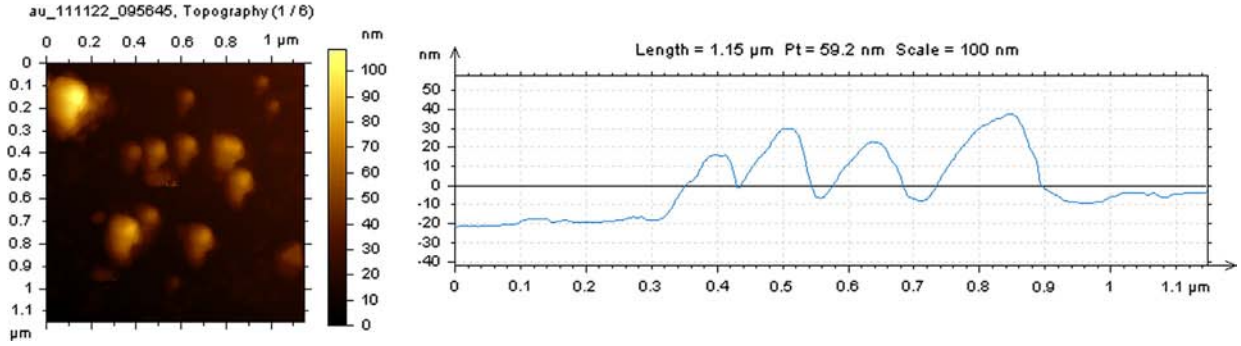

Fig. 4. AFM image of the gold nanoparticles deposited on silicon wafer and dried measured in tapping mode with a resonance frequency 190 kHz and a force constant 48 Nm^{-1}. The right figure shows a representation of the topography of an image cross section of the picture.

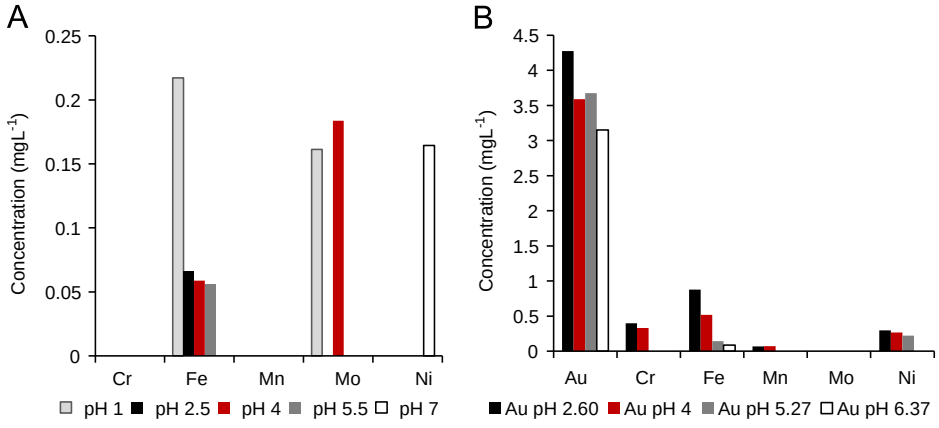

Fig. 5. Inductively coupled plasma optical emission spectroscopy (ICP-OES) analysis of metals determined in aqueous solutions of (A) HCl, and (B) $HAuCl_4$ at different pH levels after insertion of a stainless steel substrate.

3.6. *Stability of bare gold nanoparticles*

A main characteristic of nanoparticles is that the number of atoms at the surface is higher than the number of internal atoms. Consequently, the stability of NPs depends on the number of surface atoms, i.e., for stable equilibrium conditions there must be sufficient atoms at the surface to stabilize the colloid (providing charges), yet enough atoms within the nanoparticle core to

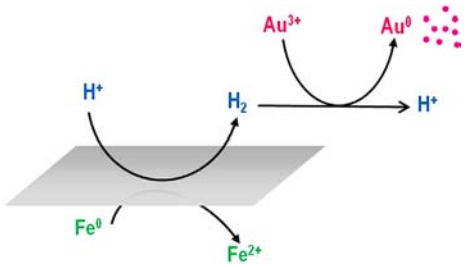

Fig. 6. Proposed scheme of stainless steel mediated AuNPs synthesis mechanism.

provide the required thermodynamic stability. Apparently, the conditions provided by the present synthetic rout facilitates slow AuNP growth until an optimal size is achieved, thus enabling stable positively charged gold nanoparticles with a narrow size distribution.

As an exceptional feature of this novel synthesis strategy, the obtained gold nanoparticles proved to be stable if stored at 4 °C for over four months. At room temperature, thus obtained AuNPs slowly precipitate at the bottom of the vial (i.e., the solution still remains stable over a period of approximately 20 days) due to agglomeration. During conventional AuNPs synthesis using e.g., citrate as reducing agent, an additional clean-up step is required for removing residual ligands. It has been described that the stability of thus purified 20-nm AuNPs synthesized with citrate is 20 days stored at 4 °C in darkness, and that aggregates are already observed after 6 days of storage at room temperature [15]. Thus, the AuNPs stability against aggregation achieved with the present method is improved as compared to conventional citrate reduction after ligand removal. The presence of ions in solution, which may interact with the positively charged nanoparticles, will influence their stability. While there are no citrate ligands present in the synthesis bound to the nanoparticle surface, chloride ions are in abundance, and may shield thus obtained nanoparticles. It is thus hypothesized that a chloride shell prevents nanoparticle agglomeration and facilitates the stabilization of the solution due to the achieved spacing between individual NPs. Finally, low ionic strength media support the stability of NPs in solution [35], which is also the case during the present synthesis.

3.7. Analytical potential of bare gold nanoparticles

Gold nanoparticles have been extensively related to Analytical Science and Technology in two complementary approaches. On the one hand, they have been the objects of the analysis by applying a variety of analytical techniques for their characterization, as it has been shown in the previous sections of this paper.

On the other hand, gold nanoparticles have been successively used as useful tools to implement a variety of functions in (bio) chemical measurement processes (i.e. as components of electrodes, as SERS substrates, as components of (bio)sensors, etc).

Two great advantages of the use of bare gold nanoparticles as analytical tools arise from the fact that there are not potential interferences from the excess of reductant used in their synthesis than act as ligands (i.e. citrate) in the suspension; and that those bare gold nanoparticles are produced with a narrow size distribution. Thus, two crucial analytical properties attributed to analytical processes involving gold nanoparticles are enhanced: selectivity and precision.

The analytical potential of these novel bare gold nanoparticles as SERS substrates has been proved. They enable the determination of carboxylated single walled carbon nanotubes by surface enhanced Raman scattering (SERS) spectroscopy mediated by the nanoparticles. The enhancement factor, calculated from the Raman

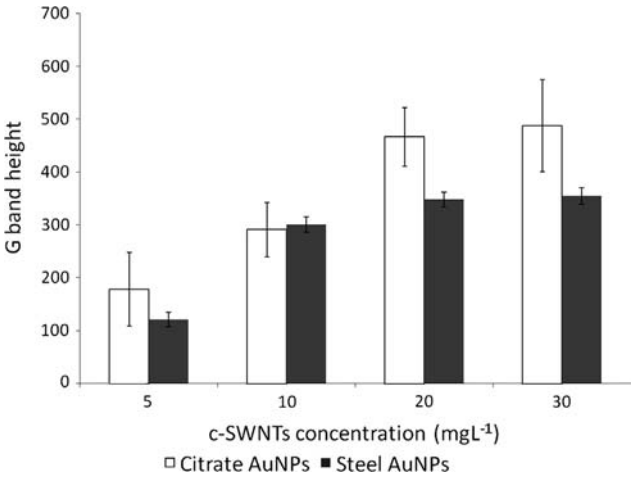

Fig. 7. Comparison of SERS response, in terms of carbon nanotube G band height, at different concentrations of c-SWNTs provided by citrate-coated and stainless steel assisted synthesized gold nanoparticles.

signal of 5 μL of 100 mg L^{-1} solution of c-SWNTs compared to that obtained when 5 μL of a 8 mg L^{-1} solution is placed on gold nanoparticles substrate, was found to be 39 ± 1.

The analytical results obtained from two analytical processes involving citrate surrounded and bare gold nanoparticles as SERS substrates were compared. The same analytical procedure was carried out with the two types of gold nanoparticles. As it can be seen in Fig. 7, at higher carbon nanotube concentrations citrate gold nanoparticles showed a slightly better performance in terms of enhancement, although the reproducibility of those membranes were less accurate, being observed small aggregates of nanoparticles.

The similar behavior observed for citrate reduced gold nanoparticles and those obtained through the proposed methodology suggest that they are suitable for being used as SERS substrate for the determination of several analytes in different analytical applications.

4. Conclusions

The main contribution of this paper is the use of a solid reducing agent –a stainless steel piece- which can be recovered from the solution, for the production of bare gold nanoparticles. The process is simple and easily scalable. 20 nm size, nearly spherical shaped nanoparticles are obtained, which have been characterized by SEM, TEM, AFM and EDX analysis. Our approach leads to bare gold nanoparticles without any ligand in their surface, obtained through an inexpensive and environmentally friendly synthesis procedure avoiding the use of harsh chemicals. A highlight of the procedure is that leads to highly stable gold nanoparticles –for more than four months when stored at 4 °C- despite the absence of stabilizing ligands on their surface, just mediated by the chloride ions present in solution which may shield thus obtained nanoparticles.

Gold nanoparticles obtained through this novel procedure are good candidates for be used as SERS substrate since they showed a similar behavior than that synthesized with citrate when applied to the SERS determination of carboxylated carbon nanotubes. The use of these bare gold nanoparticles in Analytical Science and Technology provides analytical processes with enhanced sensitivity and selectivity, owing to their stability, the absence of potential interferences from the excess of reductant and their narrow size distribution.

Acknowledgments

A.I. López-Lorente, B.M. Simonet, and M. Valcárcel wish to thank Spain's Ministry of Innovation and Science for funding Project CTQ2011-23790 and Junta de Andalucía for Project FQM4801. A.I. López-Lorente also wishes to thank the Ministry for the award of a FPU Research Training Fellowship (Grant AP2008-02939), and gratefully acknowledges funding of her stay in Germany at the University of Ulm to conduct the research reported in this paper. The authors also thank the Focused Ion Beam Center UUlm at the University of Ulm for SEM and EDX measurements.

References

[1] R.A. Rippel, A.M. Seifalian, J. Nanosci. Nanotechnol. 11 (2011) 3740–3748.
[2] W. Lu, A.K. Singh, S.A. Khan, D. Senapati, H. Yu, P.C. Ray, J. Am. Chem. Soc. 132 (2010) 18103–18114.
[3] G. Cao, Nanostructures and nanomaterials. Synthesis, Properties & Applications, Imperial CollegePress, London, 2004.
[4] J. Zhou, J. Ralston, R. Sedev, D.A. Beattie, J. Colloid Interface Sci. 331 (2009) 251–262.
[5] J. Turkevich, P.C. Stevenson, J. Hillier, Discuss. Faraday Soc. 11 (1951) 55–75.
[6] G. Frens, Nature Phys. Sci. 241 (1973) 20–22.
[7] K.C. Grabar, R.G. Freeman, M.B. Hommer, M.J. Natan, Anal. Chem. 67 (1995) 735–743.
[8] H. Mühlpfordt, Experientia 38 (1982) 1127–1128.
[9] J.W. Slot, H.J. Geuze, Eur. J. Cell Biol. 38 (1985) 87–93.
[10] G. Schmid, Chem. Rev. 92 (1992) 1709–1727.
[11] M. Brust, M. Walker, D. Bethell, D.J Schiffrin, R. Whyman, J. Chem. Soc. Chem. Commun. (1994) 801–802.
[12] E.C. Stathis, A. Fabricanos, Chem. Ind. (London) 27 (1958) 860–861.
[13] A. Fabrikanos, S. Athanassiou, K.H. Leiser, Z. Naturforsch 186 (1963) 612–617.
[14] R.G. DiScipio, Anal. Biochem. 236 (1996) 168–170.
[15] S.K. Balasubramanian, L. Yang, L.Y.L. Yung, C.N. Ong, W.Y. Ong, L.E. Yu,, Biomaterials 31 (2010) 9023–9030.
[16] U. Kreibig, L. Genzel, Surf. Sci. 156 (1985) 678–700.
[17] P.L. Redmond, X. Wu, L. Brus, J. Phys. Chem. C 111 (2007) 8942–8947.
[18] N. Pernodet, X. Fang, Y. Sun, A. Bakhtina, A. Ramakrishnan, J. Sokolov, A. Ulman, M. Rafailovich, Small 2 (2006) 766–773.
[19] C. Uboldi, D. Bonacchi, G. Lorenzi, M.I. Hermanns, C. Pohl, G. Baldi, R.E. Unger, C.J. Kirkpatrick, Part. Fibre Toxicol. 6 (2009) 18.
[20] S.F. Sweeney, G.H. Woehrle, J.E. Hutchison, J. Am. Chem. Soc. 128 (2006) 3190–3197.
[21] T. Panda, K. Deepa, J. Nanosci. Nanotechnol. 11 (2011) 10279–10294.
[22] J.Y. Song, H.K. Jang, B.S. Kim, Process Biochem. 44 (2009) 1133–1138.
[23] K. Mallick, M.J. Witcomb, M.S. Scurrell, Appl. Phys. A 80 (2005) 395–398.
[24] Z. Wei, C.J. Liu, Mater. Lett. 65 (2011) 353–355.
[25] F. Mafune, J. Kohno, Y. Takeda, T. Kondow, H. Sawabe, J. Phys. Chem. B 105 (2001) 5114–5120.
[26] V. Amendola, M. Meneghetti, J. Mater. Chem. 17 (2007) 4705–4710.
[27] H. Ma, B. Yin, S. Wang, Y. Jiao, W. Pan, S. Huang, S. Chen, F. Meng, Chem. Phys. Chem 5 (2004) 68–75.
[28] V. Amendola, S. Polizzi, M. Meneghetti, J. Phys. Chem. B 110 (2006) 7232–7237.
[29] C.H. Wang, C.C. Chien, Y.L. Yu, C.J. Liu, C.F. Lee, C.H. Chen, Y. Hwu, C.S. Yang, J.H. Jeg, G. Margaritondo, J. Synchrotron Radiat. 14 (2007) 477–482.
[30] G. Merga, N. Saucedo, L.C. Cass, J. Puthussery, D. Meisel, J. Phys. Chem. C 114 (2010) 14811–14818.
[31] A.I. López-Lorente, B.M. Simonet, M. Valcárcel, Analyst 137 (2012) 3528–3534.
[32] A.I. López-Lorente, B.M. Simonet, M. Valcárcel, Talanta 105 (2013) 75–79.
[33] S. Eustis, M.A. El-Sayed, Chem. Soc. Rev. 35 (2006) 209–217.
[34] J. Feng, M. Sun, H. Liu, J. Li, X. Liu, S. Jiang, J. Chromatogr. A 1217 (2010) 8079–8086.
[35] L.A. Dykman, V.A. Bogatyrev, Russ. Chem. Rev. 76 (2007) 181–194.